Form Error Estimation Using Spatial Statistics

Tai-Hung Yang
John Jackman
Department of Industrial
and Manufacturing Systems Engineering,
Iowa State University,
Ames, IA 50011

Form error estimation is an essential step in the assessment of product geometry created through one or more manufacturing processes. We present a new method using spatial statistics to estimate form error. Using large sets of uniform sample points measured from five common machined surfaces, we compare the form error estimates using individual points and fitted surfaces obtained through spatial statistical methods. The results show that spatial statistics can provide more accurate estimates of form error under certain conditions. [S1087-1357(00)01701-9]

1 Introduction

Reconstructing a surface from a set of discrete measurements is a problem shared by a number of related fields including reverse engineering, inspection, and topography. The general approach is to fit the data to some underlying model to obtain an artificial surface. In the context of form error estimation, we can use an artificial surface to determine the form error for a given product geometry. A set of data points are obtained from the surface of a workpiece using devices such as a coordinate measuring machine (CMM). A fundamental question arises—can we fit an artificial surface to the set of points that provides a more accurate representation (in terms of form error) of the actual surface than the individual data points? If this is possible, then a more accurate estimation of form error can be obtained by evaluating the artificial surface.

Yang and Jackman [1] reviewed and evaluated current sampling strategies and sample data analysis for form error estimation. Without considering the correlation of the sample points, they modeled the probability distribution of form error for random sampling. This previous work did not take into account the correlation between neighboring locations inherent in geometric measurements.

Palanivelu et al. [2] investigated the performance of least-squares estimation and minmax estimation of simple geometries. The algorithms were tested using data sets as well as ideal geometries with induced form errors using composite sine waves and random errors. They observed that the presence of sinusoidal errors caused greater variability in the estimates. Stratified sampling performed better than random or uniform sampling.

Yan and Menq [3] described form error as a deterministic component and random component. The random error was assumed to be spatially independent with a normal distribution for uncertainty parameters representing coordinate transformation elements. They developed a theoretical envelope for the random error component. For the deterministic component, the authors proposed a two-step method in which measurements are used to construct an artificial surface. This surface is then fitted to the nominal surface and the deterministic error is estimated using the orthogonal deviation from the nominal surface. They found that the two-step method gave more accurate estimations of form error. In related work, Yang and Menq [4] again treated form errors as having deterministic and random error components. They developed a hypothesis test for determining spatial independence. If the null hypothesis is rejected, then deterministic error is assumed to be present. For the deterministic method, an iterative fitting approach is proposed to successively fit a B spline of increasing order until the null hypothesis is accepted (i.e., spatial independence after taking into account deterministic error).

Contributed by the Manufacturing Engineering Division for publication in the JOURNAL OF MANUFACTURING SCIENCE AND ENGINEERING. Manuscript received May 1997; revised Aug. 1999. Associate Technical Editor: C. H. Menq.

Kurfess et al. [5] proposed a method for calculating confidence intervals based on the assumption that dimensions on a part have a multivariate normal distribution. A two-stage method is proposed in which deterministic errors are accounted for by first fitting a known deterministic model. The confidence intervals are estimated from the deviations from the fitted model. The challenge in this approach is to find the appropriate deterministic model.

In this paper, we consider this spatial dependence between sample points by using spatial statistics, especially the universal kriging method, in the estimation of form errors. The surface data used in these studies are from the *Atlas of Machined Surfaces* [6]. We would like to thank Dr. P. J. Sullivan for sending us these data. The region for each surface is a square with sides measuring 1.304 mm. The grid spacing on both axes was 8 μm, giving a total of 26,896 (164×164) data points for each sample.

2 Spatial Statistics for Form Error Estimation

Let the set of all points on a surface being measured be denoted by

$$\{Z(s):\ s\in D\},$$

where s is a spatial location vector in R^2 (a two-dimensional reference datum plane). The index set D defines a finite region on the surface. We obtain a set of measurements, $\{Z(s_1),\ldots,Z(s_n)\}$, at known locations $s_1,\ldots,s_n$.

Previously, Yang and Jackman [1] characterized the surface of a workpiece using a beta distribution for the deviation from nominal with the assumption that the measurements were sufficiently far apart so that $Z(s_1),\ldots,Z(s_n)$ were treated as independent of each other. However, for most surfaces the values of $Z(s)$ at locations in close proximity tend to be related to each other. The covariance function

$$\mathrm{cov}(Z(s_i),Z(s_j))=C(s_i,s_j)\quad \forall s_i,s_j\in D, \tag{1}$$

describes the relationship between the values $Z(s_i)$ and $Z(s_j)$ at locations s_i and s_j. If $C(s_i-s_j)$ is a function only of $\|s_i-s_j\|$ (i.e., the distance between the points), then the surface (characterized by $C(\cdot)$) is called isotropic. Surfaces are anisotropic if the dependence between $Z(s)$ and $Z(s+d)$ is a function of both the magnitude and the direction of d so that the variance is no longer purely a function of the distance between two spatial locations. A random function $Z(\cdot)$ having a covariance function as in Eq. (1) and

$$E(Z(s))=\mu\quad \forall s\in D, \tag{2}$$

is called second-order (or weak- or wide-sense) stationary.

The variogram is an important parameter of geostatistics that is also used to describe the relationship between values at two locations. The variogram

$$\mathrm{var}(Z(s_i)-Z(s_j))=2\gamma(s_i-s_j)\quad \forall s_i,s_j\in D. \tag{3}$$

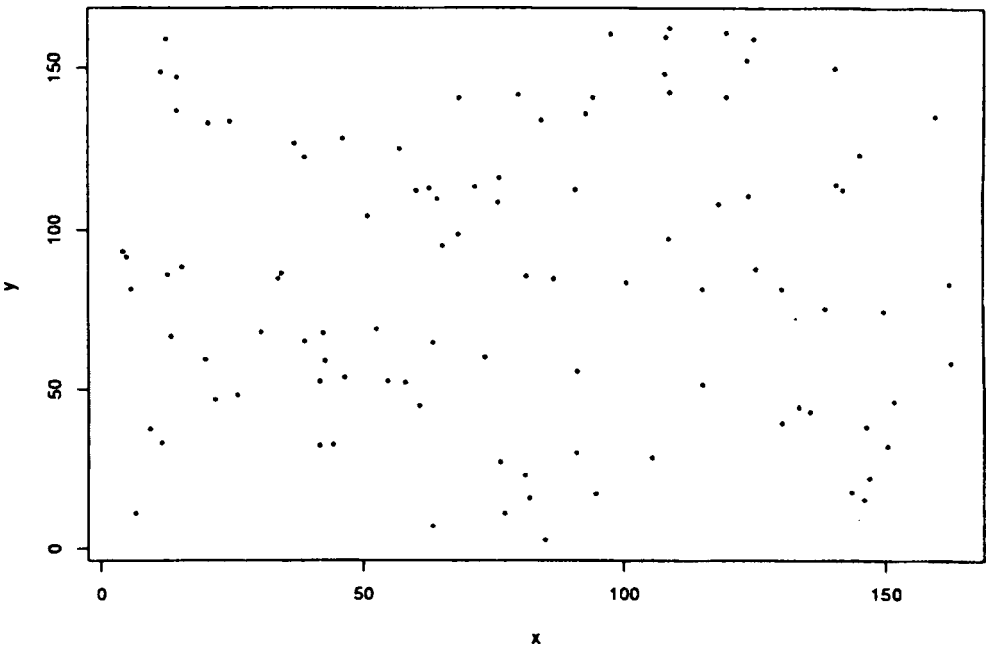

Fig. 1 Sample points (100) taken from the bored surface

represents the variance of the difference between Z values at different locations. The function $\gamma(\cdot)$ is called a semivariogram. When the process is second-order stationary, $C(\cdot)$ and $\gamma(\cdot)$ are related by

$$\gamma(h)=C(0)-C(d).$$

Note that $C(0)=\text{var}(Z(s))$ is the variance of $Z(s)$ at any location s. Cressie [7] points out that the variogram exists even for some processes that are not second-order stationary, and hence, is more general than the covariance function. The majority of machined surfaces are typically anisotropic because they exhibit a pronounced lay or directional character. Sayles and Thomas [8,9] also point out the limitations of $C(\cdot)$ and use the structure function

$$S(h)=E\{[Z(s)-Z(s+d)]^2\},$$

to model the spatial dependence in their surface roughness studies.

Assuming that a process is stationary with respect to the mean (i.e., Eq. (2) holds), then $\text{var}(Z(s+d)-Z(s))=E(Z(s+d)-Z(s))^2$ and the variogram is estimated by

$$2\hat{\gamma}(d)=\frac{1}{n_d}\sum_{(i,j)\|s_i-s_j\|=d}(Z(s_i)-Z(s_j))^2, \tag{4}$$

where the summation is over all distinct pairs of locations in the sample that are separated by distance d, and n_d is the total number of pairs separated by d. Other robust estimations of variogram are also described in Cressie [7]. For irregularly spaced data, pairs of data with approximately the same separation may be grouped together. Finally, a smooth curve (e.g., linear, exponential, spherical, rational quadratic model) is fitted to the set of variogram estimates for a discrete set of values in order to interpolate the variogram values for other distances.

2.1 Kriging. Kriging is a stochastic processes prediction theory used to produce contour maps of surfaces derived from regularly or irregularly scattered points in a space. This theory uses $C(\cdot)$ or $\gamma(\cdot)$ in the prediction process. If we assume a process is second-order stationary (i.e., Eq. (2) holds), then ordinary kriging can be used to predict the process. If the process is isotropic, then estimator (4) can be used. However, if the process is anisotropic, the variogram estimators are not only a function of distance but also a function of direction (i.e., $\gamma(d,\theta)$ in polar coordinates). Cressie [7] gives an important note about the variogram estimators. If μ in Eq. (2) is not constant but in fact depends on the location s, then the variogram estimators are actually estimating

$$2\gamma(d)+(E(Z(s+d))-E(Z(s)))^2.$$

Thus, if the process is nonstationary (i.e., Eq. (2) does not hold), we can decompose the process into two components

$$Z(s)=\mu(s)+\varepsilon(s),$$

where $E(Z(s))=\mu(s)$ and $\varepsilon(s)$ is a zero-mean intrinsically stationary stochastic process with $\text{var}(\varepsilon(s+d)-\varepsilon(s))=\text{var}(Z(s+d)-Z(s))=2\gamma(d)$. The $\mu(s)$ component represents a deterministic trend surface that accounts for large-scale variation. The $\varepsilon(s)$ component represents small-scale variation on the trend surface and is considered to be stochastic in nature. An example of a trend surface $\mu(s)$ used in kriging is

$$\mu(s)=a+c(x)+r(y), \quad s=(x,y)', \tag{5}$$

where a is the overall trend, c is a column effect, and r is a row effect. Another example is

$$\mu(s)=\sum_{u+v\leq p}a_{uv}x^u y^v, \quad s=(x,y)', \tag{6}$$

where integer p is the order of the trend surface.

Expression (5) is the basis of median-polish kriging and Eq. (6) is the basis of universal kriging [7]. The general approach is to estimate the trend surface $\mu(s)$ and subtract it from the data values $\{Z(s_i)\}$ to obtain residuals $\{\varepsilon(s_i)\}$. The residuals are treated as stationary and a variogram is fitted to the residuals. Finally, the estimated residuals are combined with the trend surface to obtain estimates of the actual surface.

Venables and Ripley [10] provide a software package in SPLUS [11] to implement universal kriging. The minimum mean-square-error unbiased predictor $\hat{Z}(x)$ is given by Ripley [12] as

$$\hat{Z}(s_0)=f(s_0)^T\hat{\beta}+y^T k(s_0). \tag{7}$$

The computation procedure is summarized as follows:

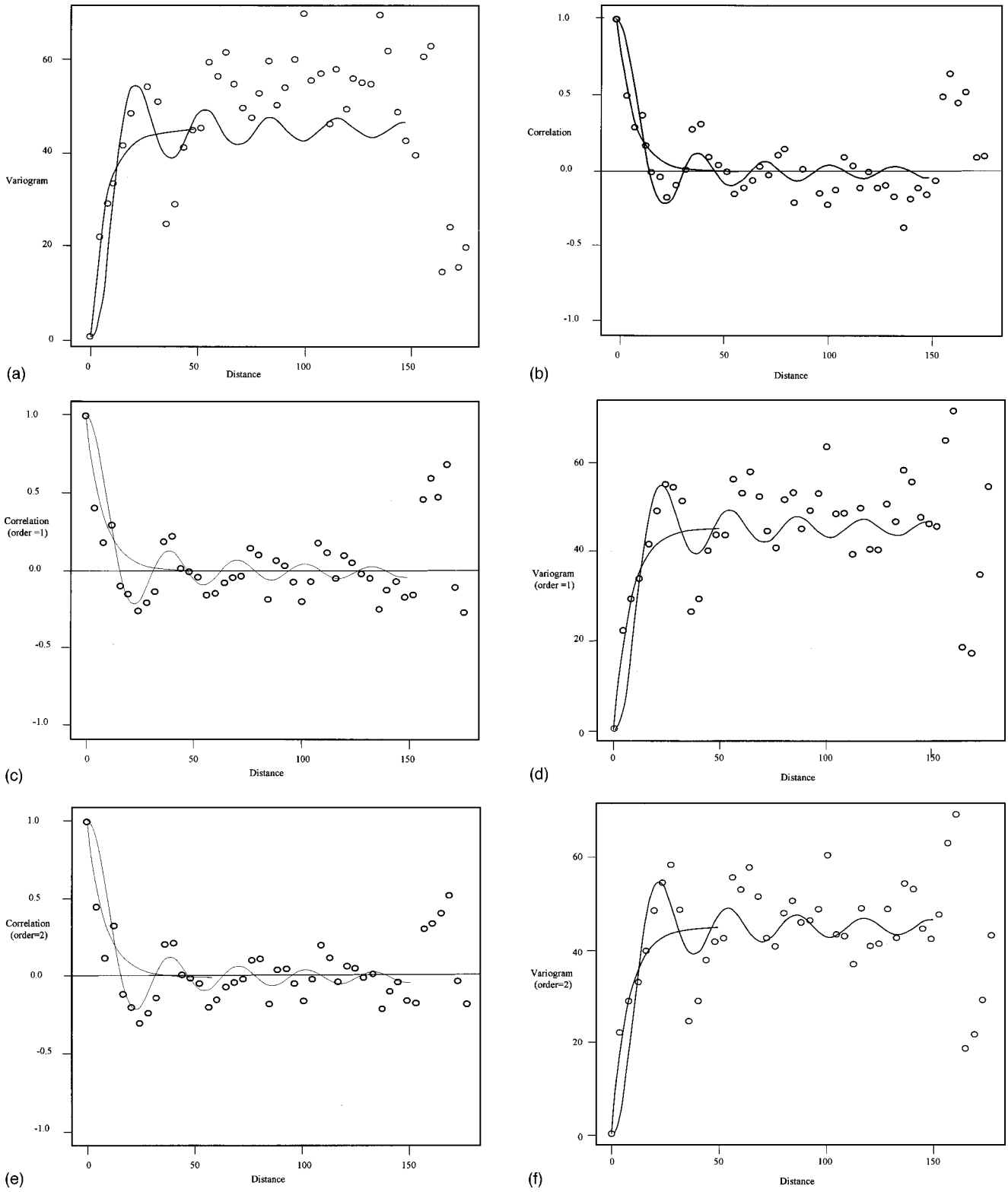

Fig. 2 Variograms and correlograms for 100 data points. (*a*) and (*b*) Sample points; (*c*) and (*d*) residuals from first-order surface; and (*e*) and (*f*) residuals from second-order surface.

1 Form $K=[C(s_i,s_j)]$.

2 Find L such that $LL^T=K$, where LL^T is the Cholesky decomposition of K and L is a lower triangular matrix.

3 Form

$$F=\begin{bmatrix} f_1(s_1) & \cdots & f_P(s_1) \\ \vdots & & \\ f_1(s_1) & \cdots & f_P(s_N) \end{bmatrix} \quad \text{for} \quad Z_N=\begin{bmatrix} Z(s_1) \\ \vdots \\ Z(s_N) \end{bmatrix},$$

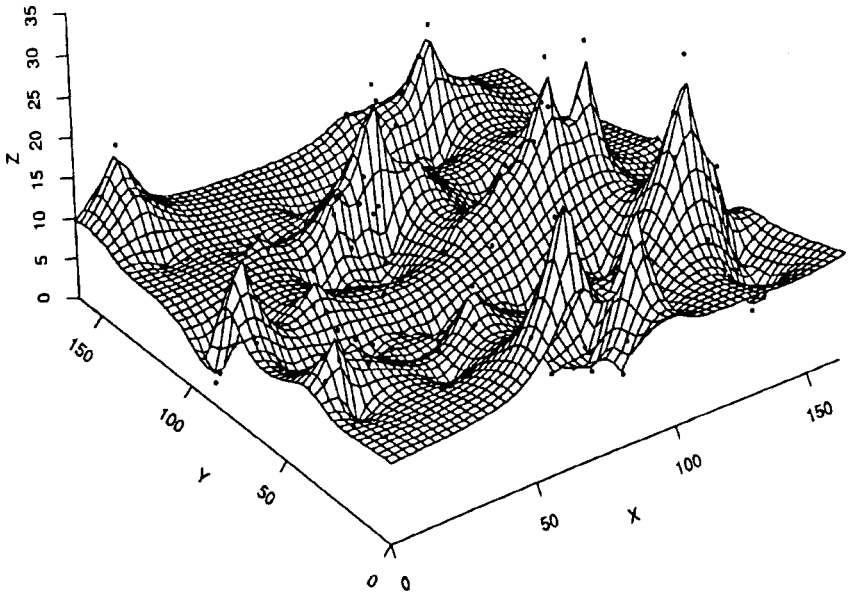

(a)

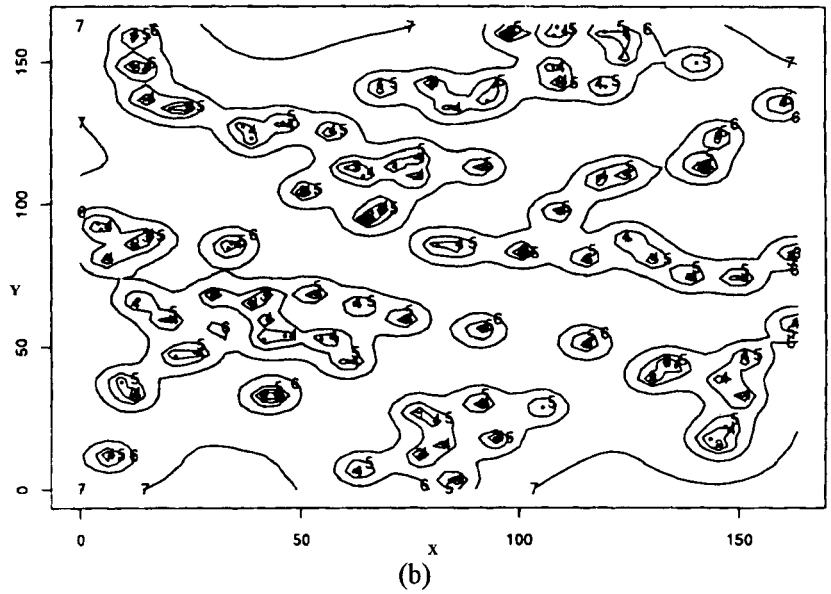

(b)

Fig. 3 Fitted surface (*a*) and standard error of the prediction error (*b*) for exponential model with $a_e=8$.

where f is polynomial function for the trend surface and P is the number of coefficients $P=(p+1)(p+2)/2$, where p is the order of the trend surface.

4 Solve $L^{-1}Z_N=L^{-1}F\hat{\beta}$ by least squares for $\hat{\beta}$.

5 Form $W_N=[Z(s_i)-f(s_i)^T\hat{\beta}]$.

6 Find y such that $L(L^Ty)=W_N$.

7 Predict $Z(s_0)$ by $f(s_0)^T\hat{\beta}+y^Tk(s_0)$, where $k(s_0)=[C(s_0,s_i)]$ and $\text{var}(Z(s_0)-\hat{Z}(s_0)]=C(s_0,s_0)-\|e\|^2+\|g\|^2$, where $Le=k(s_0)$, $R^Tg=f(s_0)-(L^{-1}F)^Te$, and R is the orthogonal reduction of $L^{-1}F$.

3 Method for Form Error Estimation Using Kriging

We will not consider the extrapolation of the fitted surface which is outside the convex hull (CH) formed by the sample points in the $X-Y$ plane, i.e., $\hat{Z}(s)$ with $s\in$ CH only. Our procedure to calculate the flatness error by using universal kriging is described as follows:

1 Take random samples $Z(s_1),\ldots,Z(s_N)$ from the inspected surface.

2 Use Venables and Ripley's programs to calculate $\hat{Z}(s)$ and σ_E^2 within D. Note that the grid size specified in their program in X and Y directions to obtain the surface coordinates will affect the approximation of the flatness errors of the predicted surface.

3 Obtain the two-dimensional (2D) convex hull only considering X and Y coordinates of the sample points. QHULL [13] can be used to find 2D or three-dimensional (3D) convex hulls for a given set of points.

4 Remove the fitted surface outside the convex hull of the $X-Y$ plane.

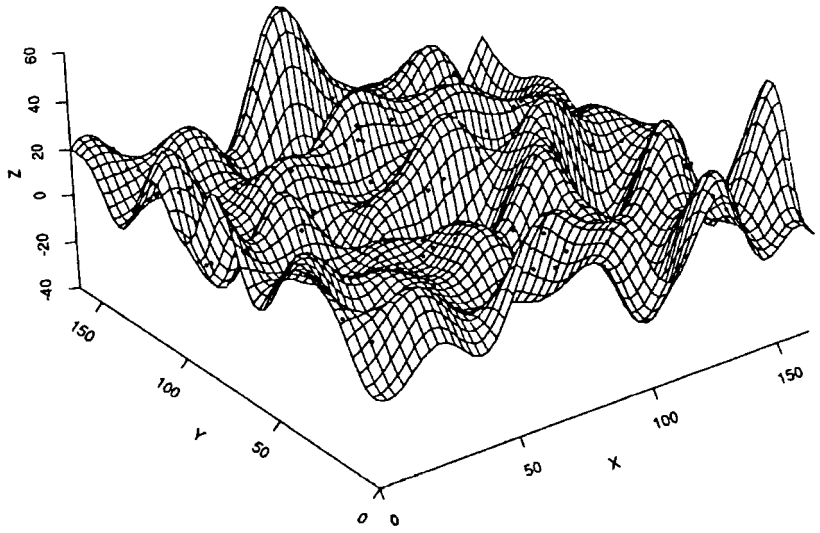

(a)

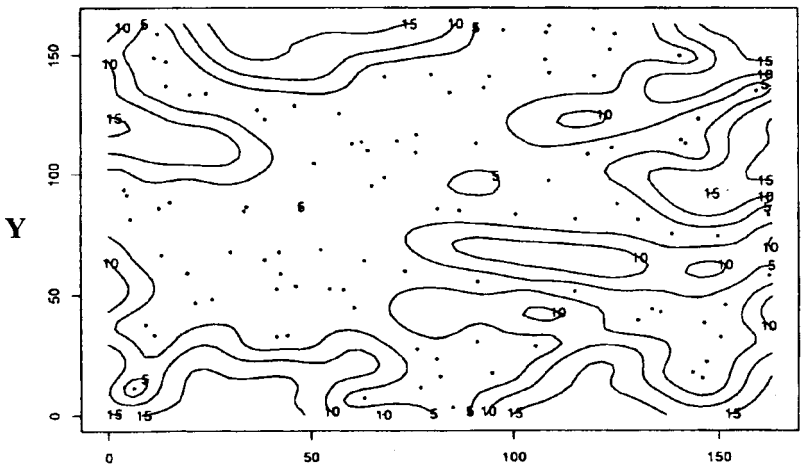

(b)

Fig. 4 Fitted surface (*a*) and standard error of the prediction error (*b*) for wave model with $a_w=5$

5 Calculate the flatness error of the fitted surface ($X-Y$ coordinates) inside the convex hull CH.

Note that a similar procedure could be used for the estimation of other form, orientation, and position error zones.

3.1 Flatness Error Estimation for a Surface From a Boring Process. As an example of form error estimation, we illustrate the use of universal kriging to calculate the flatness error for a machined surface from a boring process. An estimate of flatness error (using the minmax method in Yang and Jackman [1]) is 41.16 using all 26,896 points. We treat this estimate as the true flatness error which would be unknown to the inspector. Let us define an inspection process where we take 100 sample points from this surface (i.e., the set of 26,896 points) using a random sampling method. The scatter plot of these points in the $X-Y$ plane is shown in Fig. 1. If we only consider the individual points, the flatness form error (using the minmax method as before) is 29.31. Next we use universal kriging to generate an artificial surface for these points.

The variogram must satisfy a property called conditional negative definiteness, i.e.,

$$\sum_{i=1}^{m}\sum_{j=1}^{m} a_i a_j 2\gamma(s_i-s_j)\leqslant 0,$$

for any finite number of spatial locations $\{s_i:\ i=1,...,m\}$ and real numbers $\{a_i:\ i=1,...,m\}$ satisfying $\Sigma_{i=1}^{m} a_i=0$. Otherwise, we may obtain negative mean-squared errors of prediction. The variogram estimators, e.g., $\hat{\gamma}(d)$, cannot be used for kriging because they are not necessarily conditionally negative definite. It is suggested that a variogram model be selected from among a parametric family of variograms which best fits the data [7]. Figure 2 shows correlation plots for the data and the residuals from first- and second-order surfaces using Eq. (6), together with covariance functions fitted by the eye (the fitting of correlation (variogram) function is a subjective process). The covariance functions used are the exponential model

$$C(d,a_e)=-e^{-\|d\|/a_e}, \tag{8}$$

and wave model

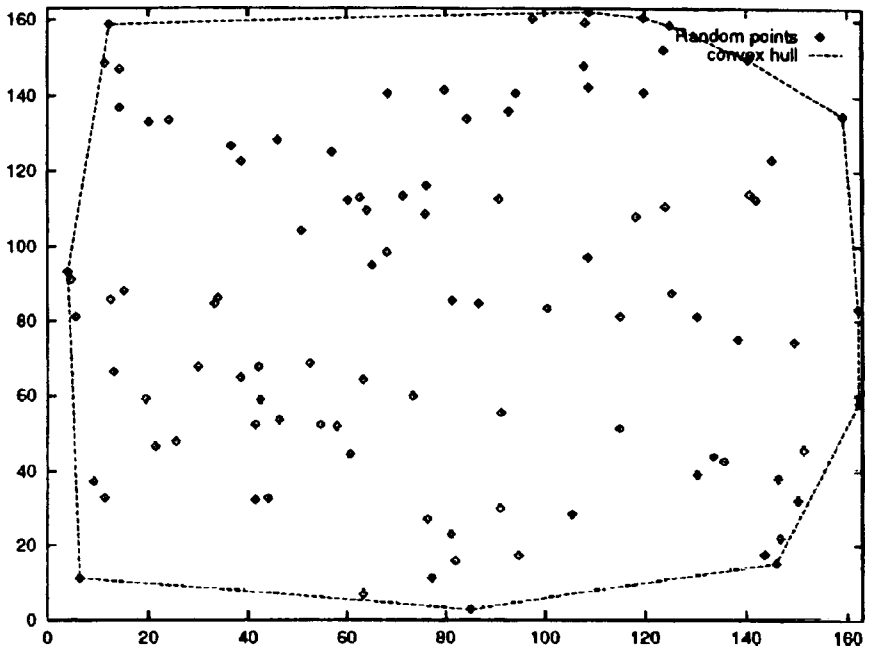

Fig. 5 Convex hull (CH)

$$C(d,a_w)=a_w\frac{\sin(\|d\|/a_w)}{\|d\|}. \tag{9}$$

The corresponding variogram models are

$$\gamma(d,a_e,b_e)=b_e[1-e^{-\|d\|/a_e}], \tag{10}$$

and

$$\gamma(d,a_w,b_w)=b_w\left[1-a_w\frac{\sin(\|d\|/a_w)}{\|d\|}\right], \tag{11}$$

for the exponential model and the wave model, respectively. The parameters (a_e,b_e) and (a_w,b_w) must be estimated for each model.

If $\gamma(h)\to c_0>0$ as $h\to 0$, then c_0 is called the nugget effect, which is caused by measurement error. Since we consider the measurement error to be negligible, the nugget effect is not included in these covariance functions. That is, the correlation is 1.0 when the distance is 0.0, which will result in the krigged surfaces going through those measurement points. As seen in Figs. 2(*c*)–2(*f*), introducing a trend surface makes little difference in these correlograms.

As can be seen from Fig. 2, even with a relatively large number of data points, it is difficult to fit the variogram and covariance models. The exponential model in Fig. 2(*b*) drops off quickly as the distance between two points increase. The wave model in Fig. 2(*b*) has the same rapid drop-off followed by a decreasing oscillation. However, to say that either of these models is a good fit for the points would be an exaggeration at best. Figures 3 and 4 show the predicted surfaces and the prediction standard errors for these two models fitted in Fig. 2 without the trend surface. The fitted covariance model parameters are $a_e=8$ and $a_w=5$. As can be seen from the two surfaces, the choice between different covariance models (exponential and wave models) makes a significant difference in prediction.

Although the fitted surfaces are continuous, we use a 55×55 sample grid within the region D to approximate this fitted surface. Since we do not consider the extrapolation of the fitted surface, we find the convex hull for the sample points in region D, which is shown in Fig. 5. Only the grids inside the convex hull are used in the program to determine the flatness error. The flatness error (using the minmax method on the grid values) is 25.54 for Fig. 3 (exponential model), which is smaller than 29.31 obtained by using individual points, or 62 percent of the true value. Because we use a rectangular grid to represent the predicted surface and calculate the flatness error, the results can be biased low because we may miss the minimum and maximum points. Figure 4 gives a large flatness error of 72.28, which is 76 percent larger than the true error 41.16 calculated from all 26,896 points.

3.2 Implications for Form Error Estimation. De-trending the data is an important issue in kriging. Universal kriging is limited to polynomial trend surfaces. Cressie [7] suggests that median-polish kriging can provide a more flexible and statistically resistant method of spatial prediction than universal kriging. Another more serious concern is the choice of a variogram model (covariance function), which can make a large difference in prediction as we saw in the preceding example. We see from the previous example that incorrectly fitting the wave model results in an overshoot for predicted surfaces. Also, it is recommended that the variogram fitting should use only up to half the maximum possible lag and then only using lags for which $n_d>30$ [7]. Thus, the empirical variogram fitted from the sample data usually needs a large number of samples. It is also important to have a good fit for the variogram at small distances between data points due to the spatial dependence. In sampled data analysis, nothing can be said about the variogram at lag distances smaller than $\min\{\|s_i-s_j\|:\ 1\leq i<j\leq N\}$. For a small number of sample points, this poses a significant problem.

After performing universal kriging on a number of different

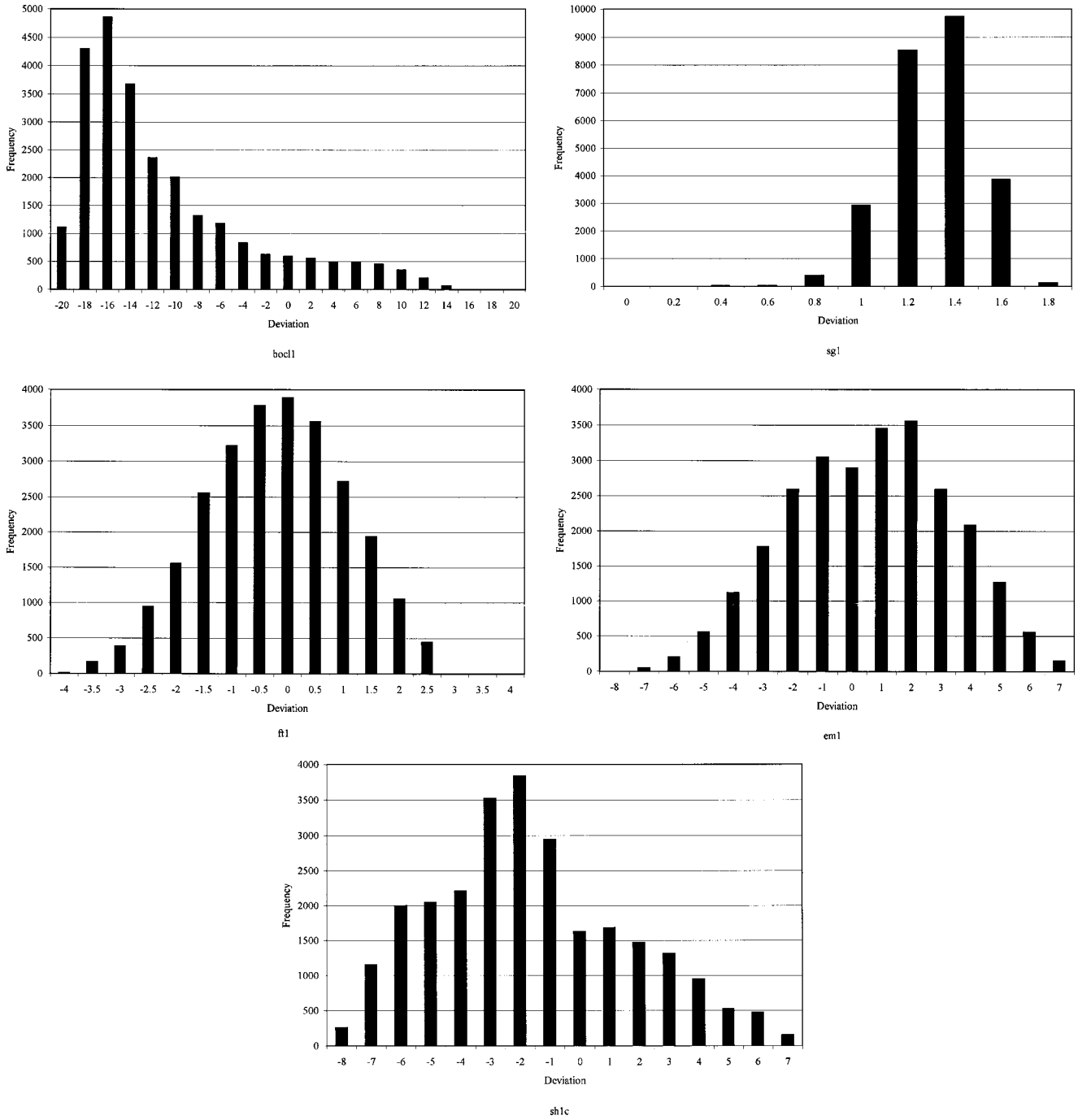

Fig. 6 Histogram of deviations from minimum zone mean profile

Table 1 Parameters of beta distribution and flatness errors

Surface	a	b	α	β	Flatness errors ($\times 10^{-2} mm$)
bocl1	-20.589	20.812	1.090	3.033	41.16
em1	-9.108	8.658	5.041	3.760	17.31
ft1	-3.866	3.975	4.091	4.158	7.68
sg1	-1.953	1.968	1.527	6.898	4.40
sh1c	-8.014	8.005	2.020	2.678	15.98

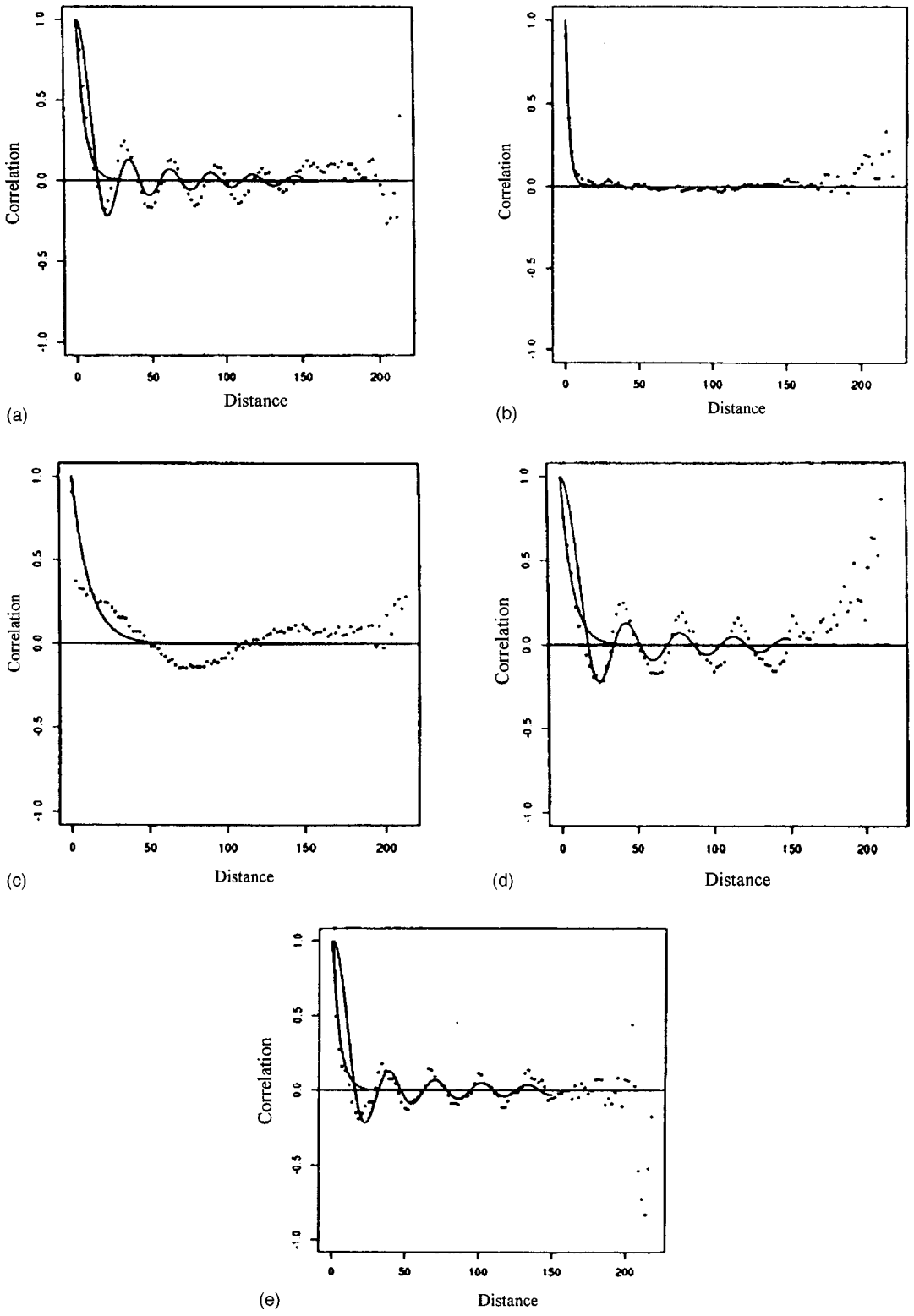

Fig. 7 Correlograms obtained from 1000 points on each surface. (*a*) End milling; (*b*) grinding; (*c*) fly cut; (*d*) boring; and (*e*) shaping.

surfaces, we found the following phenomenon. The variogram determines whether the predicted surface falls inside or outside the 3D convex hull of the data points. If the slope of the variogram approaches zero as the distance approaches zero, kriging will return values which may be outside the 3D convex hull. If the variogram has a slope which is sufficiently greater than zero when the distance is zero, the resulting interpolated value will lie within the 3D convex hull. Therefore, the commonly adapted exponential model (the spatial dependence getting smaller as the distance increases) will always result in a predicted surface within the 3D convex hull. This is an unfavorable situation since this provides no additional information to standard interpolation.

Table 2 Parameters of exponential and wave models

Surface	a_e (exponential model)	a_w (wave model)
bocl1	7.0	5.5
em1	5.0	4.4
ft1	10.5	N/A
sg1	2.5	N/A
shlc	5.0	5.0

3.3 Sampling Considerations. The only sampling method discussed to this point is uniform random sampling. Ripley [12] evaluated the performance of uniform random sampling, stratified random sampling, and uniform (systematic) sampling on the estimation of the mean value within region D. He calculated variance of the error of mean-value estimation, $N\,\mathrm{var}[\Sigma Z(s_i)/N - \int_D Z(s)ds/\text{area of D}]$, and found that if there is strong local positive correlation, both stratified random and systematic sampling should do well relative to uniform random sampling. He further concluded that uniform (systematic) sampling should be the best with smaller error variance unless the process has strong periodicity with a wavelength corresponding to the basic sampling interval along either axis or with a wavelength along a diagonal. In this paper, we confine our discussion to uniform sampling strategies.

4 Flatness Estimation for Machined Surfaces

The data in this study come from common machining processes, namely, end milling (em1), grinding (sg1), fly cut (ft1), boring (bocl1), and shaping (shlc). Each machining process produces a surface with its own characteristic topography. We use these five surfaces to evaluate universal kriging for estimating flatness errors under the uniform sampling situation.

4.1 Random Sampling. The minimum zone mean profile is the estimated plane in the middle of the flatness error zone. By enclosing all the sample points with two planes parallel to this mean profile, we can find the flatness error zone. We estimate the mean profile using all 26,896 points for each surface and use these results for the true value of flatness. The histograms of the deviations from minimum zone mean profile are shown in Fig. 6. As can be seen from the histograms, the surfaces differ both in magnitude and distribution of the deviations from the mean profile.

Table 1 shows the parameters of beta distribution for these deviations and the (true) flatness error for each surface as calculated using the minmax method.

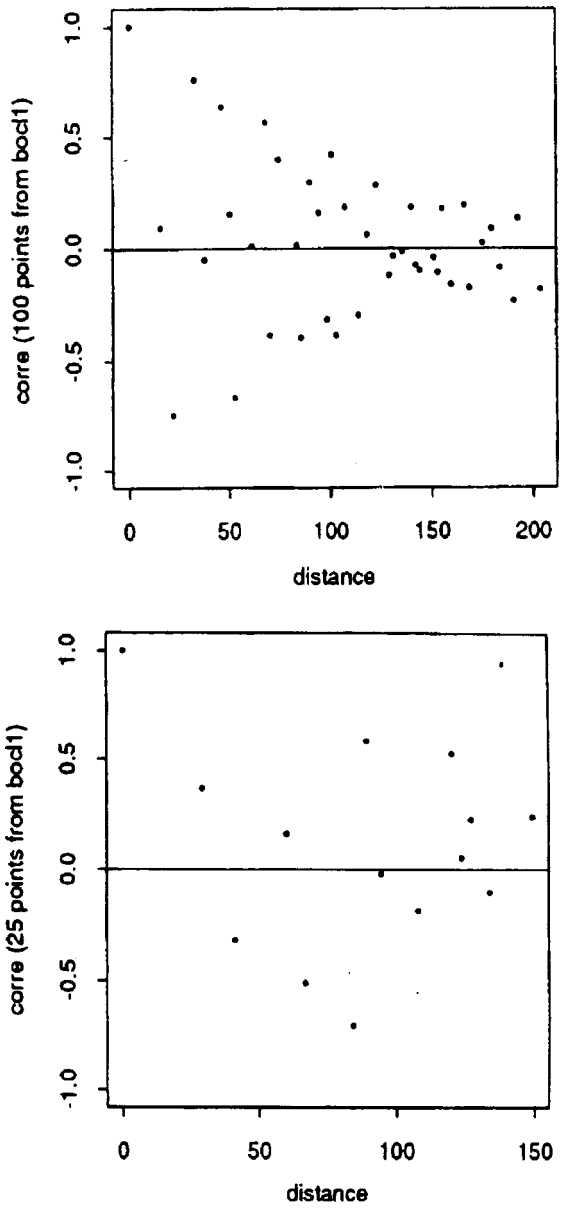

Fig. 8 Correlograms of 100 and 25 points from boring surface

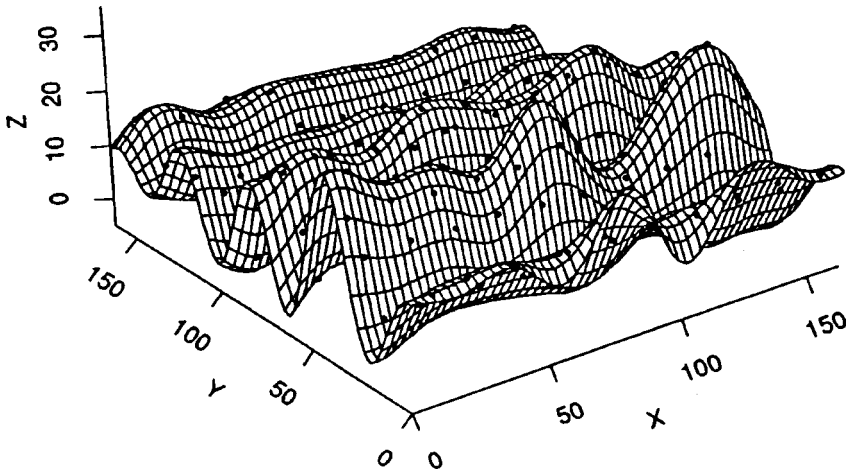

Fig. 9 Universal kriging result of 100 sampling points taken from surface bocl 1

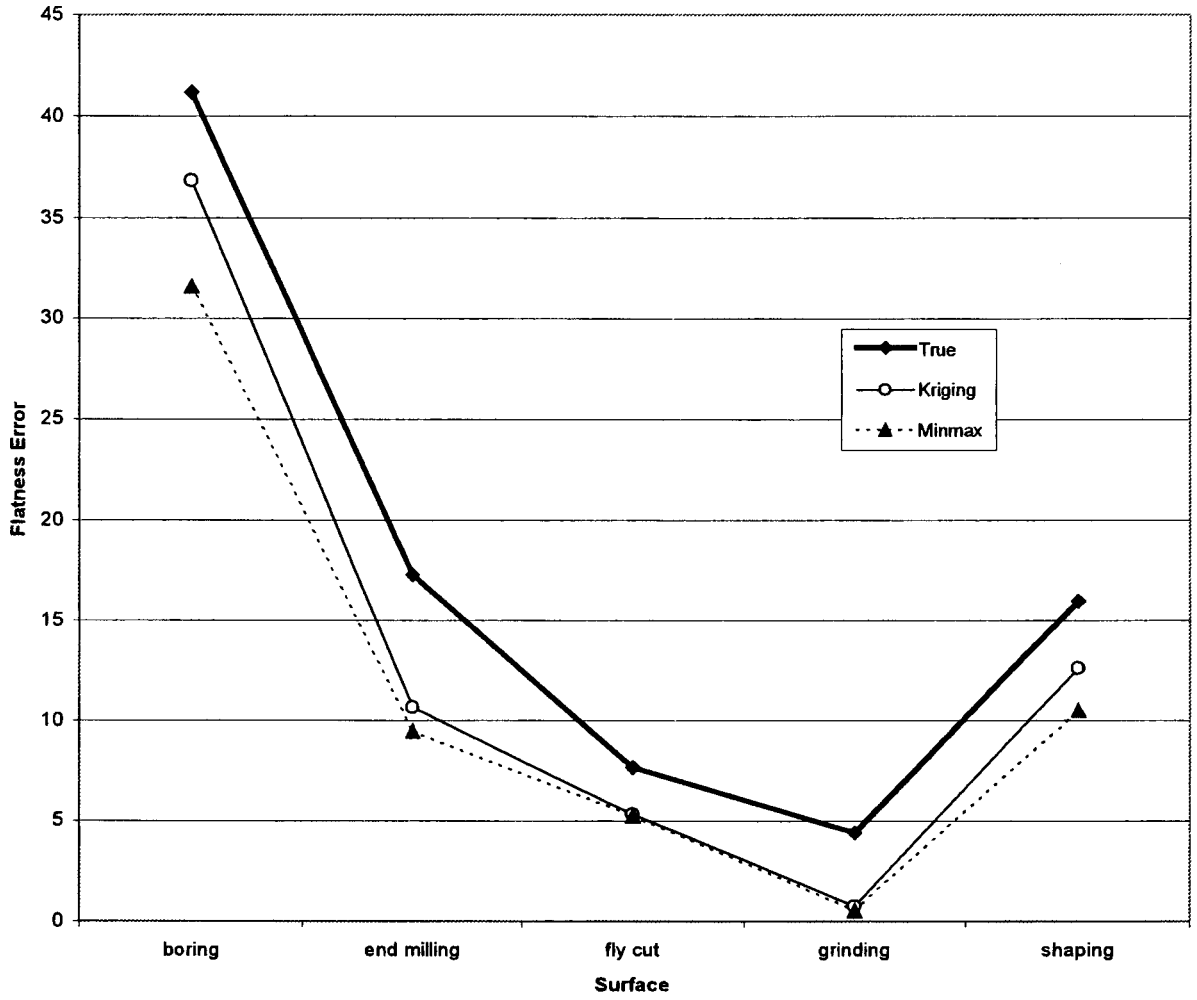

Fig. 10 Flatness error estimation

4.2 Universal Kriging. As we discussed in Sec. 2, the empirical correlogram (variogram) is hard to identify and fit when we have a small number of sampling points. If we take 1000 random sample points from these five surfaces and draw the correlograms, we see some obvious wave correlation patterns between spatial locations for surfaces bocl1, em1, and shlc, as shown in Fig. 7. The ft1 and sg1 surfaces follow more of an exponential model.

Table 2 lists the parameters of exponential and wave models obtained by fitting the correlation functions by eye to these surfaces. In contrast to these clear correlation patterns drawn from a large number of samples, the correlation patterns are difficult to identify for a small number of sample points.

To demonstrate the difficulty of fitting the correlogram or variogram with smaller sample sizes, we show the correlograms of 100 and 25 uniform sampling points taken from the bocl 1 surface in Fig. 8. The points shown in the correlogram plots are $n_d > 6$ pairs for a given distance d, which is greatly relaxed from the recommended $n_d > 30$. Given the difficulty of fitting these variograms, we use the models listed in Table 2 (obtained from 1000 sample points) as a priori correlation functions for universal kriging in this comparative study.

The fitted surfaces are then discretized and the flatness errors are calculated from these discrete points. Figure 9 shows an example of the fitted surfaces by universal kriging from 100 sample points on the boring surface. The flatness errors are summarized in Fig. 10.

Based on this study, we make the following observations:

1 Since many machined surfaces have pronounced lay and direction character (i.e., strong periodicity), the sampling period should avoid the surface periodicity as noted by Ripley [12]. If we take this into account when we perform uniform sampling with a small number of samples, the result should be better (higher detectability and lower standard deviation) than random sampling, which has larger standard errors when a small number of samples is taken.

2 The form errors estimated by kriging are equal to or greater than those calculated by single points for most of the surfaces. (Note: however, this is not the case for exponential models used by universal kriging. The krigged surfaces lie within the 3D convex hull, which agrees with the observation we made in Sec. 3.)

3 Kriging provides a standard deviation map for the artificial surface. How to utilize this error information to characterize the mean and standard deviation of form error estimation for a given number of uniform sampling points on general surfaces requires further study.

5 Conclusions

We have shown how spatial statistics can be used to estimate form errors. This method takes into account spatial dependence

between sample points. A large number of samples (on the order of 1000 samples) is required to make this method feasible. The method consists of the following steps.

1 Measure a set of points on a surface.
2 Estimate the parameters for the variogram model.
3 Fit the kriged surface.
4 Sample points from the kriged surface.
5 Use the minmax method to estimate form errors.

Our results indicate that the use of this method performs as well as using the points directly and in some cases outperforms this direct method. Identifying and fitting a correct variogram model (covariance function) from the sample points is a critical step in the estimation process. Due to the uncertainty in the variogram estimation, it is recommended that this method be used when a large number of samples are available. Given the periodicity of some of the machined surfaces, sampling should be performed at a frequency higher than those observed on a surface.

A major advantage of kriging is that it provides a map for estimates of prediction error for the fitted surface. Conceivably, it would be possible to create some form of a confidence interval for the surface. This could be used in an iterative method to identify areas on the surface that may require more measurements.

The artificial surfaces generated by fitting the sample points to a kriging model can be used to reconstruct a surface which may be of interest in applications where the nature of the surface geometry is of more interest than the dimensional characteristics of the surface.

References

[1] Yang, T. H., and Jackman, J., 1997, ''A Probabilistic View of Problems in Form Error Estimation,'' ASME J. Manuf. Sci. Eng. **119**, No. 3, pp. 375–382.
[2] Palanivelu, D., Hari, Y., Chen, K., Yang, J., Raja, J., and Hocken, R., 1991, ''Testing of Algorithms for Coordinate Measuring Machines,'' *Proceedings of the International Precision Engineering Seminar Joint International Conference of the 6th Precision Engineering and the 2nd Ultraprecision in Manufacturing Engineering*, May 1991, Secaucus, NJ, pp. 82–84.
[3] Yan, Z., and Menq, C., 1995, ''Uncertainty Analysis for Coordinate Estimation Using Discrete Measurement Data,'' *Proceedings of Manufacturing Science and Engineering*, **1**, pp. 595–616, ASME International Mechanical Engineering Congress and Exposition, November 12–17, 1995, San Francisco, CA.
[4] Yang, B., and Menq, C., 1993, ''Compensation for Form Error of End-Milled Sculptured Surface Using Discrete Measurement Data,'' Int. J. Machine Tools Manuf., **33**, pp. 725–740.
[5] Kurfess, T., Banks, D., and Wolfson, L., 1996, ''A Multivariate Statistical Approach to Metrology,'' ASME J. Manuf. Sci. Eng., **118**, pp. 652–657.
[6] Stout, K., Davis, E., and Sullivan, P., 1990, *Atlas of Machined Surfaces*, Kluwer Academic Publishers, London, U.K.
[7] Cressie, N., 1993, *Statistics for Spatial Data*, Revised Edition, Wiley, New York, NY.
[8] Sayles, R. S., and Thomas, T. R., 1977, ''The Spatial Representation of Surface Roughness by Means of the Structure Function: A Practical Alternative to Correlation,'' Wear, **42**, pp. 263–276.
[9] Sayles, R. S., and Thomas, T. R., 1979, ''Measurements of the Statistical Microgeometry of Engineering Surfaces,'' J. Lubr. Technol., **101F**, pp. 409–418.
[10] Venables, W. N., and Ripley, B. D., 1994, *Modern Applied Statistics with S-Plus*, Springer, New York, NY.
[11] Becker, R. A., 1988, *The New S Language: A Programming Environment for Data Analysis and Graphics*, Pacific Grove, CA: Wadsworth & Brooks/Cole Advanced Books & Software.
[12] Ripley, B. D., 1981, *Spatial Statistics*, Wiley, New York, NY.
[13] Barber, C. B., Dobkin, D. P., and Huhdanpaa, 1993, *The Quickhull Algorithm for Convex Hull*, Technical Report No. GCG53, The National Science and Technology Research Center for Computation and Visualization of Geometric Structures, University of Minnesota.